

CHEMISTRY

A European Journal



Accepted Article

Title: Development of a library of thiophene-based drug-like LEGO molecules: evaluation of their anion binding, transport properties and cytotoxicity

Authors: Paulo Vieira, Margarida Q. Miranda, Igor Marques, Sílvia Carvalho, Li-Jun Chen, Ethan N. W. Howe, Carl Zhen, Claudia Y. Leung, Michael J. Spooner, Bárbara Morgado, Odete A. B. Cruz e Silva, Cristina Moiteiro, Philip A. Gale, and Vítor Félix

This manuscript has been accepted after peer review and appears as an Accepted Article online prior to editing, proofing, and formal publication of the final Version of Record (VoR). This work is currently citable by using the Digital Object Identifier (DOI) given below. The VoR will be published online in Early View as soon as possible and may be different to this Accepted Article as a result of editing. Readers should obtain the VoR from the journal website shown below when it is published to ensure accuracy of information. The authors are responsible for the content of this Accepted Article.

To be cited as: *Chem. Eur. J.* 10.1002/chem.201904255

Link to VoR: <http://dx.doi.org/10.1002/chem.201904255>

Supported by
ACES

WILEY-VCH

Development of a library of thiophene-based drug-like LEGO molecules: evaluation of their anion binding, transport properties and cytotoxicity

Paulo Vieira,^[a] Margarida Q. Miranda,^[b] Igor Marques,^[b] Sílvia Carvalho,^[a] Li-Jun Chen,^[c] Ethan N. W. Howe,^[c] Carl Zhen,^[c] Claudia Y. Leung,^[c] Michael J. Spooner,^[d] Bárbara Morgado,^[e] Odete A. B. da Cruz e Silva,^[e] Cristina Moiteiro,^{*[a]} Philip A. Gale,^{*[c]} Vítor Félix^{*[b]}

Abstract: The anion binding and transport properties of an extensive library of thiophene-based molecules are reported. Seventeen bis-urea positional isomers, with different binding conformations and lipophilicities, were synthesized by the appendage of α -, β -thiophene or α -, β -, γ -benzo[*b*]thiophene motifs to the *ortho*-phenylenediamine central core, yielding six subsets of positional isomers. Through ¹H NMR, X-ray crystallography, molecular modelling and anion efflux studies, it was demonstrated that the most active transporters display a pre-organised binding conformation able to promote the recognition of chloride using urea and C-H binding groups in a cooperative fashion. Additional LUV based assays, carried out under electroneutral and electrogenic conditions, together with NMDG-Cl assays, indicate that anion efflux occurs mainly through H⁺/Cl⁻ symport mechanism. On the other hand, the most efficient anion transporter displays cytotoxicity against tumour cell lines while having no effects on a cystic fibrosis cell line.

Introduction

Ion transport across phospholipid cell membranes is crucial to several biological processes, such as nerve conduction and homeostasis maintenance, being mediated by a combination of embedded protein ion channels.^[1] The dysfunction of these channels causes serious pathologies, commonly designated as channelopathies, including types of male infertility and the genetically inherited disease cystic fibrosis (CF), caused by a defective transmembrane transport of the bicarbonate and chloride anions.^[1-2]

Most of the current treatments for CF aim to manage the disease symptoms, while the cure remains a challenge. Therefore, the search for an effective treatment is of paramount importance, with CFTR modulation,^[3] and channel replacement therapies being possible pathways.^[2] Potential natural products that could be used in the latter approach are restricted to the pamamycins,^[4] duramycins,^[5] prodigiosins,^[6] and, more recently, amphotericin B.^[7] This unselective channel was shown to restore lung cell's ability to secrete HCO₃⁻, thus enhancing the antibiotic activity of the airway surface liquid and reducing its viscosity.^[7] Still, the development of a myriad of small drug-like molecules capable of mediating the selective transmembrane anion transport is still imperative, being a field of intensive research.^[8] Most of these molecules have been designed translating the know-how acquired with the development of anion receptors,^[9] coupling natural^[10] or synthetic platforms with suitable binding units, that operate *via* conventional or non-conventional hydrogen bonds,^[11] *via* halogen,^[12] chalcogen,^[13] or pnictogen bonding interactions,^[13c] or even through anion- π interactions.^[14] Beyond anion binding strength, the anion transport ability of a synthetic receptor is also largely dependent of its ability to partition into the lipid bilayer, *i.e.* its partition coefficient, and can be tuned by the addition of structural motifs with different lipophilicities, such as alkyl chains, aromatic groups and fluorinated units.^[15] Moreover, there is growing evidence that synthetic anionophores are also able to trigger apoptosis (or disrupt autophagy) in cancer cell lines, opening a new application perspective for these anion transporters.^[10b, 16] In spite of all these achievements, the development of molecules that can make the bench-to bedside translation process is still in a relatively early stage.^[17]

The main goal of our anion transport endeavour is the development of anion carriers containing heteroaromatic moieties widely used in drug design and with the eventual goal of using these systems as Channel Replacement Therapies. From a variety of heteroaromatic fragments, the thiophene and benzo[*b*]thiophene motifs, present in different classes of drugs (*e.g.* antihistamines and analgesics),^[18] were selected. These entities have octanol-water partition coefficients ($\log P$) comparable to their benzene and naphthalene isosteres (1.81 – thiophene vs. 2.13 – benzene; and 3.12 – benzo[*b*]thiophene vs. 3.34 – naphthalene),^[19] but possess distinct electronic properties, as can be seen from the distribution of the electrostatic potential on the molecular surface (V_s) presented in Figure 1. The presence of the sulfur atom in thiophene and benzo[*b*]thiophene results in these entities being electron deficient, with the V_s in front of to the C $_{\alpha}$ -H bonds being higher than for the C $_{\beta}$ -H ones. Moreover, the anisotropic distribution of electron density around the sulfur atoms yields two σ -holes nearly aligned with the C-S bonds. The

- [a] P. Vieira, Dr. S. Carvalho, Prof. C. Moiteiro
Centro de Química e Bioquímica, Centro de Química Estrutural,
Departamento de Química e Bioquímica
Faculdade de Ciências, Universidade de Lisboa, Campo Grande
1749-016 Lisboa, Portugal.
E-mail: cmmoiteiro@fc.ul.pt
- [b] M. Q. Miranda, Dr. I. Marques, Prof. V. Félix
Department of Chemistry, CICECO – Aveiro Institute of Materials,
University of Aveiro
3810-193, Aveiro, Portugal.
E-mail: vitor.felix@ua.pt
- [c] Dr. L.-J. Chen, Dr. E. N. W. Howe, C. Zhen, C. Y. Leung, Prof. P. A. Gale
School of Chemistry (F11), The University of Sydney
NSW 2006, Australia.
E-mail: philip.gale@sydney.edu.au
- [d] Dr. M. J. Spooner
Chemistry, University of Southampton
Southampton SO17 1BJ, UK
- [e] B. Morgado, Prof. O. A. B. C. Silva
Department of Medical Sciences, Institute of Biomedicine (iBiMED)
University of Aveiro, 3810-193 Aveiro, Portugal

Supporting information for this article is given via a link at the end of the document.

FULL PAPER

chalcogen bonds derived from activated sulfur's σ -holes have been recently employed in the recognition and transmembrane transport of chloride by dithienothiophene derivatives.^[12a, 12b, 13a, 13b]

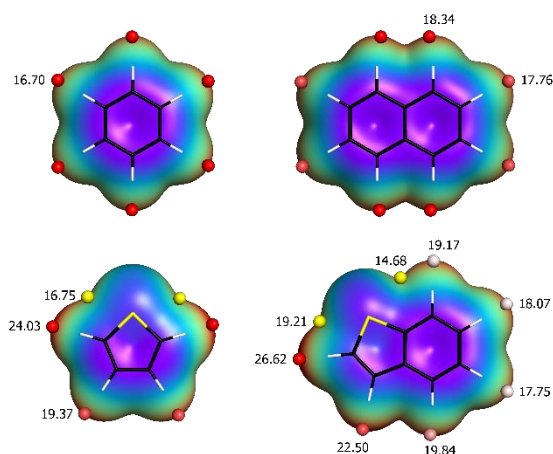


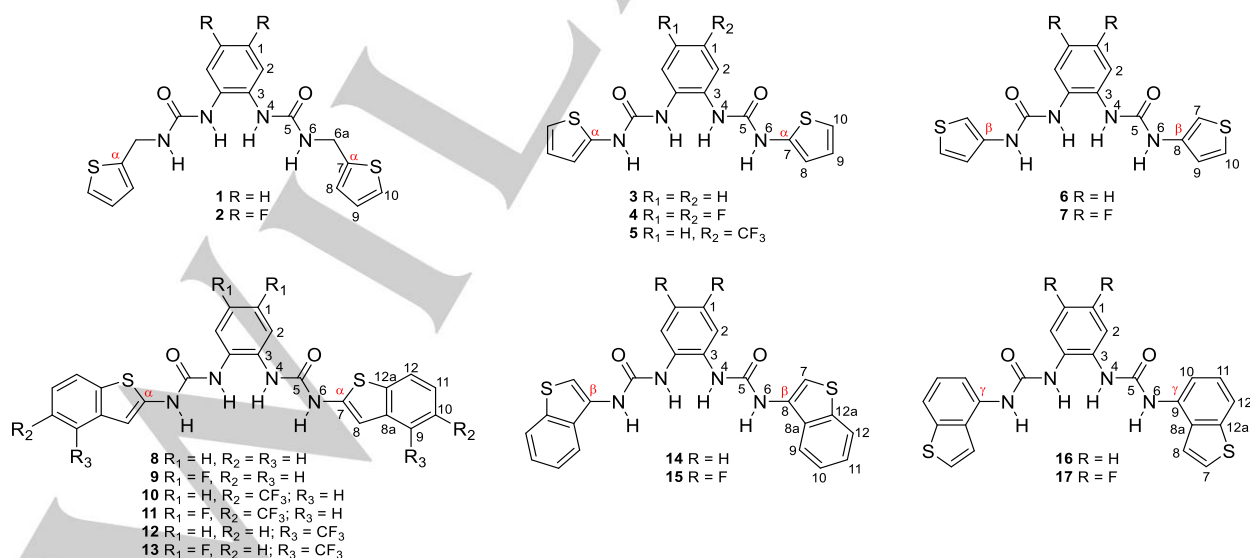
Figure 1. Comparison between the distribution of electrostatic potential mapped on the molecular surface (0.001 e Bohr⁻¹ contour) of benzene (top left), naphthalene (top right) and their respective isosteres thiophene (bottom left) and benzo[*b*]thiophene (bottom right). The colour ranges from purple (below -15.5 kcal mol⁻¹) to red (larger than 21.9 kcal mol⁻¹). The values in of the decreasing surface maxima (21.9 kcal mol⁻¹) are given along with their location in front of the C-H bonds (red, pink and salmon spheres), or at the sulfur σ -holes (yellow spheres).

Alongside the transport activity and the delivery to the cell membrane, facile synthesis is also of paramount importance in the development of drug-like anion carriers,^[20] particularly when we are interested in building and rationalising the transport properties of a large library of structurally related and chemically accessible compounds. These principles and the properties of thiophene and benzo[*b*]thiophene motifs inspired us to design a library of *ortho*-phenylene based bis-urea anion transporters

flanked with two thiophene or benzo[*b*]thiophene motifs, as depicted in Scheme 1.

This scaffold was selected due to its chemical versatility allied to its successful use in the development of anion transporters.^[21] The thiophene or benzo[*b*]thiophene moieties were directly linked to the central *ortho*-phenylene core via the C _{α} or C _{β} carbon atoms, leading to the substitution isomers α (**3**, **4**, **8**, **9**) and β (**6**, **7**, **14**, **15**), akin to assembling LEGO bricks. Moreover, the benzo[*b*]thiophene motif was also bonded to the bis-urea central core through the phenyl fused ring (C _{γ}) rather than through the thiophene, affording **16** and **17**. Furthermore, the lipophilicity and binding affinity of these molecules was mainly tuned with the fluorination of the central aromatic ring with two fluorine substituents (**2**, **4** and remaining odd numbered molecules) or a single trifluoromethyl group (**5**), while the fluorination of the phenyl fused rings distal from the bis-urea binding pocket with two electron withdrawing CF₃ groups (**10–13**) should mainly affect the molecule's lipophilicity. Whereas in all the previous molecules the heteroaromatic rings are able to communicate via the central aromatic ring, in α -thiophene derivatives **1** and **2** the methylene bridges allow to assess how the interruption of the electron delocalisation influences the anion recognition and transport properties. On the other hand, playing with the linkage positions of thiophene and benzo[*b*]thiophene substituents (C _{α} , C _{β} , and C _{γ} carbons) pre-organised conformations, stabilised by putative intramolecular chalcogen (C–S...O=C) or hydrogen (C–H...O) bonds, with different binding geometries and properties were designed, as demonstrated below.

With this library of seventeen compounds, we undertook a comprehensive investigation, comprising the molecular design assisted by computational modelling, synthesis and structural characterisation followed by experimental binding and transmembrane transport studies. Molecular dynamics simulations were also performed to obtain insights into the interaction of the thiophene-based molecules with the POPC membrane model. The cytotoxicity of the most promising anion transporters was also evaluated against cancer and CF cell lines.



Scheme 1

FULL PAPER

Results and Discussion

Molecular design and quantum descriptors

The first insights into the binding and conformational preferences of our library of molecules towards chloride were obtained through Density Functional Theory (DFT) calculations on 1:1 complexes, at the M06-2X/6-311++G(*d,p*) level of theory in a polarizable continuum model of DMSO,^[22] using Gaussian 09.^[23] The strength of the non-covalent interactions was further assessed *via* the E^2 stabilization energies through Natural Bond Orbitals (NBO) analysis.^[24]

In the α -thiophene and α -benzo[*b*]thiophene-based molecules (**3–5** and **8–13**), two conformations *A* and *B* were considered (see Scheme 2). In *A*, the spatial disposition of the thiophene rings is locked by two putative chalcogen...chalcogen bonds between the sulfur and oxygen atoms of the carbonyl groups, while in *B* the putative C–S...O=C non-covalent bonding interactions should be replaced by C–H...O ones. The optimised structures of the chloride complexes, with the receptors in alternative conformations, are shown in Figure 2 for **4** and in Figures S2 and S4 for the remaining α -thiophene and α -benzo[*b*]thiophene derivatives. In all complexes, the conformational binding arrangement *A* displays two non-covalent intramolecular bonding contacts, with S...O distances and C–S...O angles (see Table S1) consistent with the existence of chalcogen...chalcogen bonds, with an average E^2 stabilisation energy of ca. 2.6 kcal mol⁻¹, derived from the delocalization of the oxygen' lone pair to the C–S antibonding orbital ($n_o \rightarrow \sigma^*_{s-c}$). Accordingly, in the **3–5** and **8–13** chloride complexes, the conformation *A* is systematically preferred over *B*, with energy differences ($\Delta E_{cont} = E_A - E_B$) ranging from 1.9 to 2.7 kcal mol⁻¹ (see Table S2).

The chloride complexes of the β -thiophene-based molecules (**6** and **7**) were also optimised in two alternative conformations regarding the relative position of the C₇-H and C₉-H thiophene protons to the adjacent carbonyl groups (see Scheme 2 and Figure S3), due their different acidic character, measured by V_S : in conformation *A*, the C₇-H more acidic protons are close of the oxygen atoms while in *B* they are replaced by lesser C₉-H ones. Although the NBO analysis revealed the inexistence of C–H...O bonding interactions in the optimised structures of these

complexes, the binding arrangement with conformation *A* is favoured by ca. 2.1 kcal mol⁻¹.

On the other hand, the energy difference between the *A* and *B* conformations of the chloride complexes of β -benzo[*b*]thiophene derivatives **14** and **15** nearly doubles when compared with their β -thiophene-substituted complexes **6** and **7** (ca. 3.9 kcal mol⁻¹). Indeed, binding conformation *A* (Figure 2) presents a synergetic recognition of chloride *via* four classical N–H...Cl⁻ hydrogen bonds assisted by C₉-H...Cl⁻ bonding interactions (see Table S3). Moreover, in this conformation, the bonded receptors **14** and **15** are nearly planar, while in *B* they are twisted avoiding the steric clashes between the C₉ benzo[*b*]thiophenes' protons and their adjacent carbonyl groups (see Figure S5).

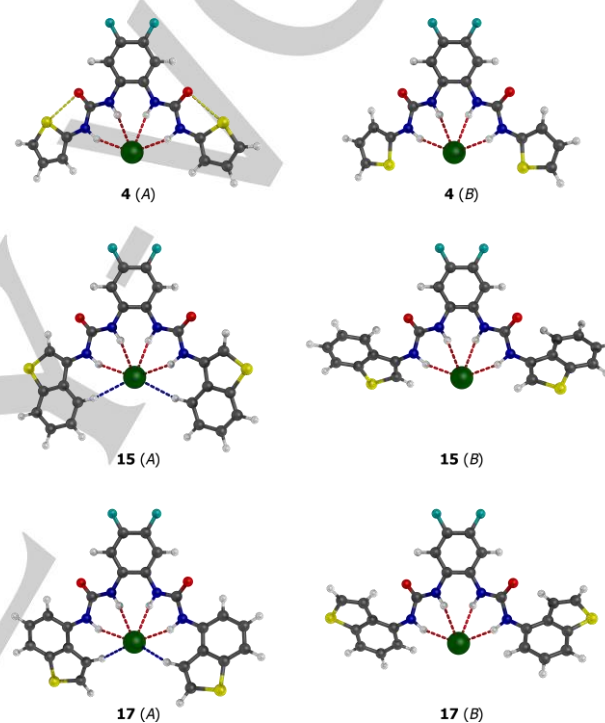
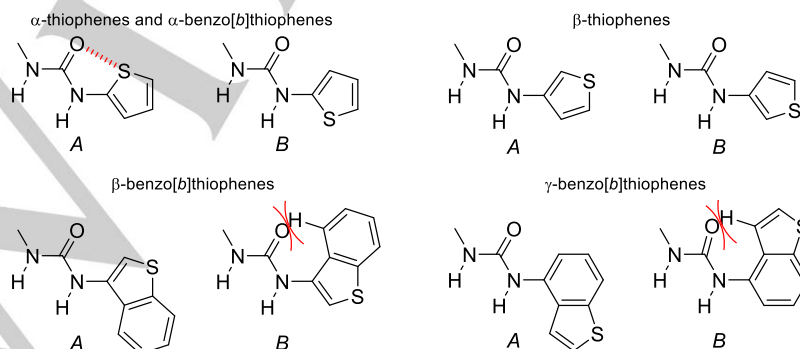


Figure 2. DFT optimised structures of the 1:1 chloride complexes of **4**, **15** and **17**, with the fluorinated receptors in the *A* or *B* conformations. The N–H...Cl⁻ and C–H...Cl⁻ hydrogen bonds are drawn in red and blue dashes, respectively, while the C–S...O=C chalcogen bonds are shown as yellow dashes.



Scheme 2

FULL PAPER

Table 1. Quantum descriptors and log*P* for bis-urea thiophene-based receptors, together with experimental binding and transport data for chloride.

Molecule	E^2 (kcal mol ⁻¹) ^a		$V_{S,max}$ (kcal mol ⁻¹) ^b	log <i>P</i> ^c	K_a (M ⁻¹) ^d	EC_{50} (mol %) ^e	k_{ini} (% s ⁻¹) ^f
	$n_{Cl^-} \rightarrow \sigma^*_{N-H}$	$n_{Cl^-} \rightarrow \sigma^*_{C-H}$					
1	28.2	2.5	94.0	3.50	31.84	- ^h	0.0345
2	29.3	2.3	102.5	3.79	44.77	- ^h	0.0383
<i>α</i> -thiophenes							
3	36.6	-	103.5	4.16	31.70	- ^h	0.0609
4	37.2	-	112.2	4.44	44.06	0.3875	0.7457
5	38.0	-	112.9	5.03	44.56	0.3604	0.7750
<i>β</i> -thiophenes							
6	34.9	- ^g	100.3	3.82	35.16	- ^h	0.0493
7	35.6	- ^g	109.1	4.11	67.61	0.3131	0.7090
<i>α</i> -benzo[<i>b</i>]thiophenes							
8	38.0	- ^g	107.5	6.35	41.02	- ^h	0.0855
9	38.5	- ^g	115.9	6.63	47.53	0.6827	0.2170
10	38.7	- ^g	115.7	8.10	57.41	- ^h	0.0347
11	39.2	-	123.9	8.39	70.79	0.4379	0.1938
12	39.5	- ^g	110.6	8.10	66.07	- ^h	0.0489
13	39.9	- ^g	119.0	8.39	74.13	- ^h	0.1792
<i>β</i> -benzo[<i>b</i>]thiophenes							
14	35.7	3.6	102.6	6.02	114.29	0.1722	0.7354
15	36.7	3.5	111.3	6.30	163.68	0.0089	4.3685
<i>γ</i> -benzo[<i>b</i>]thiophenes							
16	34.5	5.8	101.1	6.02	139.96	- ^h	0.0917
17	35.4	5.5	109.7	6.30	207.49	0.0194	1.7803

^a) Stabilization energies estimated by the 2nd-order perturbation theory; ^b) Most positive value of the electrostatic potential mapped on the molecular surface; ^c) ChemAxon Consensus log*P*; ^d) Cl⁻ added as TBA salt and the binding constants were determined by ¹H NMR titrations in DMSO-*d*₆/0.5% H₂O at 293 K using HypNMR; ^e) EC₅₀ defined as the effective concentration needed for 50% activity at *t* = 270 s; ^f) The initial rates of chloride transport (*k*_{ini}) obtained using standard Cl⁻/NO₃⁻ antiport assay for each transporter (1 mol%); ^g) *E*² < 0.2 kcal mol⁻¹; ^h) EC₅₀ not determined due to the low transport activity.

To explore the role of the C–H⋯Cl⁻ interactions in chloride binding by the benzo[*b*]thiophene motifs, the substitution isomers **16** and **17** were designed (see Scheme 1), with the decorating moieties attached to the bis-urea central core by the C_v (C₉) phenyl carbon. Likewise **14** and **15**, the DFT optimised complexes of **16** and **17** (see Figure 2) in conformation A are energetically favoured (see Table S2) and show the anion hydrogen bonded to four urea N–H binding units and two C₈–H binding units from the thiophene moieties. These C–H⋯Cl⁻ bonding contacts are ca. 0.1 Å shorter than the ones in **14** and **15** (see Table S3), affording higher *E*² stabilisation energies (ca. 2.1 kcal mol⁻¹) for **16** and **17** (see Table 1). These findings are also in line with the more acidic character of the C₈ vs. C₉ protons of the benzo[*b*]thiophene fragment (see Scheme 1 and Figure 1).

In the sequence of this energetic and structural analysis, only the computed binding arrangements with thiophene- and benzo[*b*]thiophene-derivatives adopting conformation A will be used to rationalise their binding and transport properties. Following our previous works with thiourea^[27] or squaramide-based^[16b, 28] transporters, the maximum of the electrostatic potential surface (*V*_{S,max}) was also evaluated as a binding descriptor. The *V*_{S,max} of **1-17** is located in the red binding region confined by the urea binding units, as illustrated in Figure 3 for **4**, **15** and **17** and in Figures S6 and S7 for the remaining thiophene and benzo[*b*]thiophene derivatives. The *V*_{S,max} values computed for this library of molecules (see Table 1) indicate that the fluorination of the central phenyl spacer, with the electron-withdrawing two fluorine atoms or trifluoromethyl substituents, leads to an increase of ca. 8.6 kcal mol⁻¹. On the other hand, the peripheric fluorination of the *α*-benzo[*b*]thiophene derivatives **8** and **9**, with the insertion of a trifluoromethyl group in the phenyl fused ring at position C4 (**12** and **13**) increased the *V*_{S,max} in ca.

3.1 kcal mol⁻¹, while the attachment at C5 position (**10** and **11**) affords a greater gain of ca. 8.1 kcal mol⁻¹. Overall, the *α*-thiophene and *α*-benzo[*b*]thiophene receptors with the sulfur atoms vicinal to the urea binding units, have higher *V*_{S,max} values than in their *β*-thiophene and *β*-benzo[*b*]thiophene substituted isomers. Likewise, the proximity of the sulfur atom to the urea binding units in the *β*-benzo[*b*]thiophene derivatives **14** and **15** leads to *V*_{S,max} values 1.5 kcal mol⁻¹ slightly higher than in the *γ*-benzo[*b*]thiophene isomers **16** and **17**. Moreover, the red region of positive electrostatic potential extends from the urea groups to the C–H binding units.

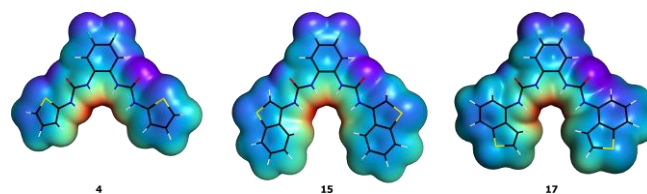


Figure 3. Distribution of electrostatic potential mapped on the molecular surface of **4**, **15** and **17** (0.001 e Bohr⁻¹ contour). The colour ranges from -34.0 (purple) to 106.4 kcal mol⁻¹ (red).

Overall, allying the chemical versatility of thiophene and benzo[*b*]thiophene motifs with the selective fluorination of the receptor skeleta (*vide supra*), we have designed a series of seventeen-synthetic drug-like molecules with different putative binding properties as well as a broad range of lipophilicities, with log*P* values ranging from 3.50 to 8.39 (see Table 1), with the isomeric ones inherently having similar lipophilic character.

FULL PAPER

Synthesis

The library of seventeen symmetrical bis-urea anion transporters (Scheme 1) was prepared by the addition of isomeric thiophene and benzo[*b*]thiophene isocyanates to *ortho*-phenylenediamine linkers with different fluorination degrees. The **1-7** molecules were obtained with high yields through one-pot synthesis using α - and β -thiophene isocyanates as provided by the chemical suppliers. The benzo[*b*]thiophene isocyanates used to produce the target molecules (**8-17**) were prepared from the corresponding carboxylic acids (see Scheme S1) which were previously converted into acyl azide intermediates, and further underwent a thermal Curtius rearrangement to yield the required isocyanates. Full synthetic details and structural characterisation data of all compounds are given in the Supporting Information.

Solid-state structures

The single-crystal structures of the free receptors **3** and **5** and halide complexes of **6**, **10**, and **12** were determined by X-ray diffraction. Suitable single-crystals of **14** for X-ray diffraction analysis were grown only from a solution containing tetrabutylammonium bromide. The structure of **14** associated with this halide is also reported.

In the crystal structure of the free α -thiophene **3**, the two urea binding units adopt a divergent spatial disposition (see Figure 4a), as result of concomitant hydrogen bonds established between them and carbonyl oxygen atoms of adjacent molecules. These hydrogen bonds, with N...O distances of 2.946(2) and 2.818(2) Å and N-H...O angles of 150 and 149°, are extended throughout the crystal lattice leading to the formation of 1D-helical chains (see Figure S53a). The crystal structure of α -thiophene **5** is generated from an asymmetric unit having two molecules of receptor (A and B) and two DMSO solvent molecules. The perspective view of the asymmetric unit of **5**, presented in (Figure 4b), shows an urea binding group of A and B assembled by N-H...O=S bridges (N...O = 2.9205(3) and 2.8075(3) Å and \angle N-H...O = 150 and 157°) and N-H...O=C hydrogen bridges (N...O = 2.8308(3) and 2.8109(3) Å and \angle N-H...O = 135 and 157°). The second binding site of B is occupied by the other DMSO crystallization molecule (N...O = 3.0086(3) and 2.8476(3) Å and \angle N-H...O = 162 and 171°), while the second binding site of A is involved in a 1D network of hydrogen bonds with B (N...O = 3.1507(3) and 2.7340(3) Å and \angle N-H...O = 137 and 152°) from neighbouring supramolecular entities, as depicted in Figure S53b. Overall, both free receptors display a divergent spatial disposition of two urea binding groups dictated by the hydrogen bonds found in solid-state, but with sulfur atoms of α -thiophene in close contact with adjacent carbonyl groups, as anticipated by the theoretical calculations (*vide supra*).

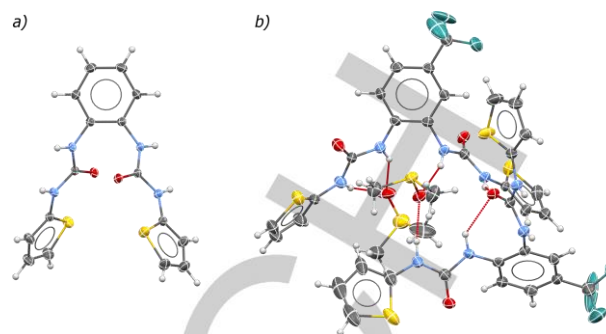


Figure 4. Perspective views of the asymmetric units of **3** (a) and **5** (b) with thermal ellipsoids drawn at the 40% probability level. The hydrogen bonds are drawn as red dashed lines.

The crystal structures of halide complexes of **6**, **12** and **14** are built from asymmetric units containing one receptor, one chloride and one TBA counter-ion. The asymmetric unit of the chloride complex of **10** is composed of two independent molecules of receptor, two chloride and two TBA counter-ions. The geometric parameters of the hydrogen bonds between the halides and **6**, **10**, **12**, and **14** are gathered in Table S6.

The structure presented in Figure 5 shows the β -thiophene derivative **6** binding the chloride in 1:1 stoichiometry through four convergent hydrogen bonds with N...Cl distances and N-H...Cl angles ranging from 2.7340(3) to 2.7340(3) Å and 137 to 162°, respectively. Furthermore, the receptor is almost planar with a dihedral angles (θ), between the planes of the *ortho*-phenyl central core and the urea binding units, of 19.1(1) and 22.4(1)°. The C7-H protons of the β -thiophene motif are close of the neighbouring carbonyl oxygen atom (H...O = 2.38 and 2.46 Å), which is consistent with preferential binding conformation (A) suggested by DFT calculations and NOESY data (*vide infra*).

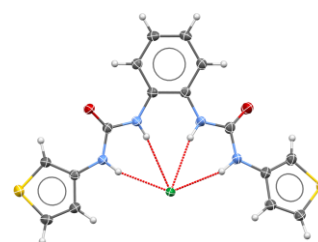


Figure 5. Molecular structure of β -thiophene **6-Cl⁻** with thermal ellipsoids drawn at the 40% probability level. The four convergent hydrogen bonds are drawn as red dashed lines.

The halide complexes of benzo[*b*]thiophene derivatives **14**, **10** and **12** display a 2:2 binding stoichiometry in the crystalline state with each halide hydrogen bonded by two urea binding units from two receptors as illustrated in Figure 6 for [12₂.Cl₂]²⁻ and [14₂.Br₂]²⁻ and in Figure S54 for [10₂.Cl₂]²⁻. These three complexes display equivalent centrosymmetric binding arrangements with two urea-binding units each single receptor adopting a divergent spatial, which contrasts with the convergent one observed in the crystal structure of β -thiophene complex **6-Cl⁻**.

FULL PAPER

Moreover, in $[\mathbf{10}_2\text{-Cl}_2]^{2-}$ and $[\mathbf{12}_2\text{-Cl}_2]^{2-}$ a urea binding unit of each receptor is twisted relatively to the *ortho*-phenyl central core with a θ angle of ca. 50° , while the other is roughly coplanar with a θ angle of ca. 30° (see Table S7). The extended α -benzo[*b*]thiophene decorating motifs are nearly coplanar with the corresponding urea binding units and the sulfur atoms are close to the carbonyl oxygen atoms at average S...O distances of 2.768(3) and 2.746(2) Å for **10** and **12**, respectively. The dimensions of the N–H...Cl⁻ hydrogen bonds, which are in good agreement with those determined for $[\mathbf{6}\text{-Cl}]^-$, as evident from the comparison presented in Table S6.

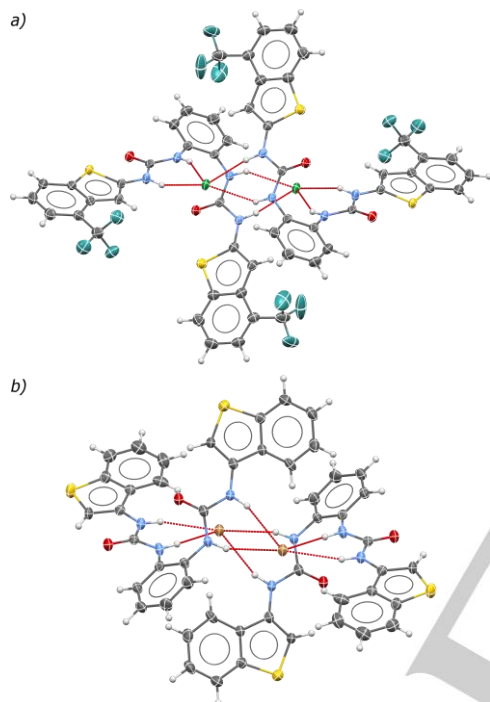


Figure 6. Molecular structures of $[\mathbf{12}_2\text{-Cl}_2]^{2-}$ (a) and $[\mathbf{14}_2\text{-Br}_2]^{2-}$ (b) with thermal ellipsoids drawn at the 40% probability level. The hydrogen bonds are drawn as red dashed lines. A -CF₃ substituent of $[\mathbf{12}_2\text{-Cl}_2]^{2-}$ is disordered over two alternative tetrahedral positions, but only the position with higher occupation factor is shown.

In centrosymmetric $[\mathbf{14}_2\text{-Br}_2]^{2-}$ the urea binding units are also twisted relatively to the *ortho*-phenyl central core by θ angles of 58.3(1) and 31.3(1) $^\circ$, while being almost coplanar with the β -benzo[*b*]thiophene decorating motifs. Moreover, the C₇-H protons of thiophene are close to the carbonyl oxygen atoms at distances of 2.33 and 2.28 Å. The four independent N–H...Br⁻ hydrogen bonds have equivalent N...Br⁻ distances, ranging from 3.4075(3) to 3.4725(3) Å, and N–H...Br⁻ angles between 141 and 162 $^\circ$.

Chloride binding studies

The chloride binding properties of our library of bis-urea derivatives were investigated by ¹H NMR experiments performed in DMSO-*d*₆/0.5% H₂O at 293 K. The binding constants were determined with HypNMR^[26] using the chemical shift variations of both internal (N₄-H) and external protons (N₆-H) of the urea binding units observed throughout the titrations with tetrabutylammonium chloride (TBACl). The ¹H NMR titration spectra are presented in Figures S56-S72. Non-linear regression analyses (Figures S73-S78) indicated a 1:1 stoichiometry for the anion complexes of **1-17**. The binding constants gathered in Table 1 show that the 4,5-difluoro-*ortho*-phenylenediamine based derivatives have systematically higher values than their non-fluorinated analogous. This finding is entirely consistent with the increased acidity of the central binding core measured by the V_{S,max} quantum descriptor (see Table 1). The impact of the fluorination degree is also evident in the complex of **5**, with a single trifluoromethyl substituent, which has a binding constant similar to difluorinated analogous **4**. The anion recognition by α -thiophene derivatives **1** and **2** occurs mainly using the N₄-H protons of the bis-urea binding units, as shown by the variations of N–H resonances upon addition of increasing amounts of chloride. Indeed, as discernible in the ¹H NMR spectra, the internal N₄-H protons present a downfield shift three and five times larger than the N₆-H ones in **1** and **2**, respectively. In contrast, the ¹H NMR spectra of α -thiophene derivatives **3-5** display comparable downfield shifts for the four urea proton resonances (ca. 0.5 ppm) while the chemical shifts of the remaining protons are almost unmoved during titrations, which indicates that the anion recognition occurs through the four convergent N–H...Cl⁻ hydrogen bonds with equivalent strength. An identical binding behaviour is apparent from the ¹H NMR titration spectra of the α -benzo[*b*]thiophene based receptors, which is expected, given the lengthened conformation adopted by **9-13** in the DFT optimised structures of their chloride complexes, with the anion away from the C₈-H protons (C₈...Cl⁻ distances are ca. 4.44 Å). In addition, in the 2D-NOESY NMR spectra of the α -benzo[*b*]thiophene substituted receptors (see Figures S83 and S84) the correlation observed between the thiophene C₈-H and urea N₆-H protons corroborates the existence of the intramolecular chalcogen...chalcogen bonding interactions found in the DFT optimised structures. In stark contrast, in β -thiophene derivatives **6** and **7**, as shown in Figures S82, both C₇-H and C₉-H are correlated with the external urea protons, showing the fluxional behaviour of these heteroaromatic rings. The chloride binding by β -benzo[*b*]thiophene **14** and **15** and γ -benzo[*b*]thiophene **16** and **17** compounds occurs with chemical shifts of the internal and external urea protons moving downfield by ca. 0.7 and 0.4 ppm, respectively. In contrast to the α -benzo[*b*]thiophene substituted receptors, significant downfield field shifts (ca. 0.4 ppm) are observed for the C₉-H phenyl ring resonances in **14** and **15** and for the C₈-H thiophene ring resonances in **16** and **17** during the titrations. This binding behaviour is illustrated in Figure 7 with titration spectra of **15** with chloride and in Figures S69, S71 and S72 for the remaining three receptors. These structural data provide evidence that the chloride is synergistically recognised by four convergent N–

FULL PAPER

H...Cl⁻ hydrogen bonds and two C-H...Cl⁻ bonding interactions. Further insights into the binding geometries adopted by these receptors in DMSO-*d*₆ aqueous solution were given by the NOESY spectra of the β- and γ-benzo[*b*]thiophene chloride complexes. The NOESY spectra of **15**, presented in Figure 8, reveals that the external protons of the urea binding units (N₆-H) correlate with the C₉-H phenyl protons, meaning that these protons are close to each other, as depicted in their DFT optimised structures (see Figure 2 and Figure S5), where the distances between protons N₆-H and C₉-H are 2.10 Å, respectively, and the H...Cl⁻ distances of 2.77 and 2.78 Å, in this order, are consistent with existence of non-conventional hydrogen bonding contacts. Likewise, in the NOESY spectra of the chloride complexes of **17** (Figure S88), the thiophene protons C₈-H correlate through the space with the external urea protons, with distance between the N₆-H and C₈-H protons of 2.18 and 2.17 Å in their respective DFT optimised geometries, which also exhibit the C-H...Cl⁻ interactions with H...Cl⁻ distances of 2.68 and 2.69 Å. Along the subsets of benzo[*b*]thiophene isomers, the binding association constants follow the order **16** > **14** > **8** and **17** > **15** > **9**, showing the paramount importance of C-H...Cl⁻ for the chloride binding strength.

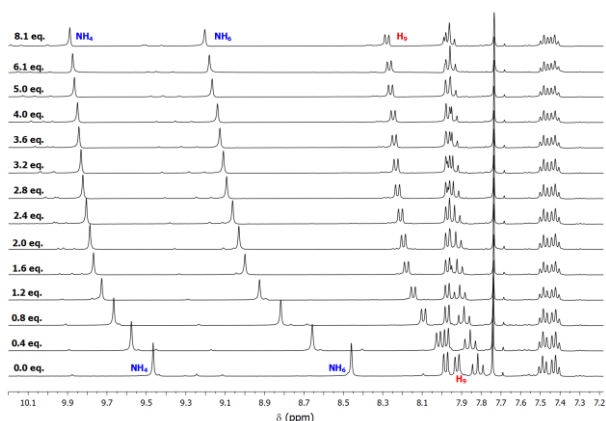


Figure 7. Selected partial (400 MHz) ¹H NMR spectra for the titration of Bu₄N⁺Cl⁻ into **15** in DMSO-*d*₆/0.5% H₂O at 293 K.

The total E^2 of the hydrogen bonding interactions (N-H...Cl⁻ and C-H...Cl⁻) are plotted against the log(K_a) in Figure S89. Apart of **1**, **2**, **6** and **7** (see Scheme 1), the molecules were grouped in two subsets: a) α-thiophene and α-benzo[*b*]thiophene derivatives; and b) β-benzo[*b*]thiophene and γ-benzo[*b*]thiophene derivatives. In the former subset, the E^2 data follow a linear relation, with an R^2 of 0.90. Noteworthy, in subset *b*, characterised by the ability of **14**–**17** to recognise chloride through cooperativity between N-H...Cl⁻ and C-H...Cl⁻ interactions, a linear relationship is also observed ($R^2 = 0.87$).

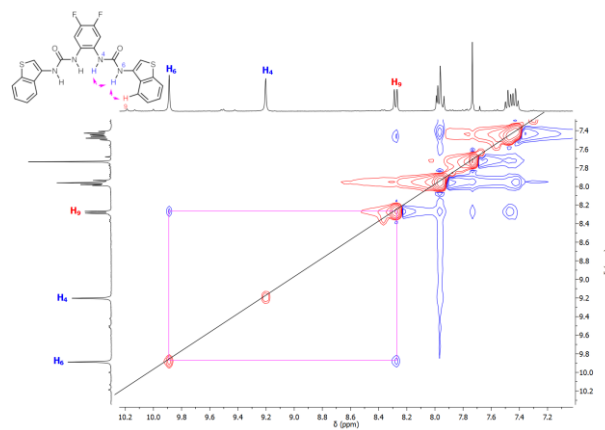


Figure 8. Close up of the 2-D NOESY spectrum of **15** (10.3 mM) with Bu₄N⁺Cl⁻ (8.1 eq) in DMSO-*d*₆ at 293 K, showing key intramolecular NOE cross-peaks (marked in magenta). NOE cross-peaks of the urea-NHs (H₄ and H₆) and H₉ were observed and marked with magenta arrows in the structure (see Figure S86 for the full spectrum).

Anion efflux studies

The anion transport properties of the new library of molecules towards chloride were determined using the chloride/nitrate exchange assay (Figure 9a) monitored by a chloride ion selective electrode (ISE). Typically, unilamellar vesicles prepared from POPC, were loaded with a buffered NaCl solution (487 mM, with 5 mM phosphate buffer at pH 7.2), suspended in a buffered NaNO₃ solution (487 mM, with 5 mM phosphate buffer at pH 7.2) and all molecules were added as a DMSO solution and the rate of chloride efflux was monitored by the chloride ISE. The initial rates of chloride transport (k_{ini}) obtained using this assay are shown in Table 1 and Figure S90. In the library of thiophene-based molecules, all non-fluorinated derivatives displayed poor chloride transport activities except β-benzo[*b*]thiophene **14**. The fluorinated molecules displayed better activities compared with their non-fluorinated analogous, indicating the lipophilicity of these molecules is an important aspect which could influence the activity of a molecule. The Cl⁻/NO₃⁻ exchange assay showed the activity sequence of **15** > **17** > **5** ≈ **4** ≈ **14** ≈ **7** > **9** ≈ **11**. The same trend was also confirmed by concentration-dependent Hill analysis (Table 1 and Figure S91-S98). The β-benzo[*b*]thiophene derivative **15** (EC₅₀ = 0.0089) is the best performing molecule, followed by γ-benzo[*b*]thiophene derivative **17** (EC₅₀ = 0.0194), benefiting from the additional C-H...Cl⁻ interactions in chloride binding by the benzo[*b*]thiophene motif.

In order to understand the behaviour and transport mechanism of these thiophene-based molecules in more detail, cationophore coupling assays (Figure 9a) were used to determine whether the receptor-mediated ion transport occurs in an electrogenic or electroneutral fashion or in a nonspecific manner. KCl-loaded unilamellar vesicles were suspended in an inert external K-Gluconate solution. Ionophore-induced Cl⁻ efflux was measured by ISE coupling with either valinomycin (an electrogenic K⁺ transporter) or monensin (an electroneutral M⁺/H⁺ transporter). As shown in Figure 9b, all tested molecules were more efficient in mediating electroneutral H⁺/Cl⁻(OH⁻/Cl⁻) than electrogenic Cl⁻

FULL PAPER

transport, and both β -benzo[*b*]thiophene derivative **15** and γ -benzo[*b*]thiophene derivative **17** appeared to be only capable of transporting chloride ions through electroneutral transport but not electrogenic transport, while the β -benzo[*b*]thiophene derivative **14** is capable of both electrogenic and electroneutral transport (Table S8 and Figure S99). Therefore, as the most two active anion transporters in this series, **15** and **17** function as electroneutral transports which promote transport *via* a pure ion pair H^+/Cl^- symport event, or *via* ion exchange.

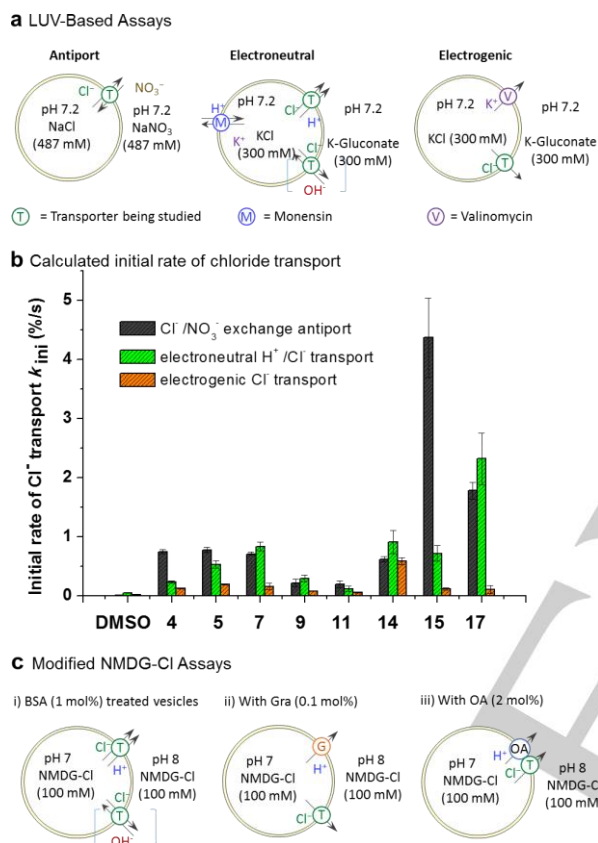


Figure 9. Overview of the anion transport ability of the thiophene-based compounds in large unilamellar vesicles (LUV). (a) Schematic lay-out of the experiments, where T = transporter, Mon = monensin, and Vln = valinomycin. (b) Initial rate of chloride transport calculated by exponential or linear fit for each transporter (1 mol%) under various assay conditions. Detail experimental conditions are presented in supporting information. (c) Schematic of the *N*-methyl-D-glucamine chloride (NMDG-Cl) assay, monitored by HPTS fluorescence: i) in bovine serum albumin (BSA) (1 mol%) treated vesicles, ii) in the presence of gramicidin (Gra) (0.1 mol%) and iii) in the presence of oleic acid (OA) (2 mol%).

Additionally, we quantified the $Cl^- > H^+/OH^-$ selectivity of these transporters using a modified *N*-methyl-D-glucamine chloride (NMDG-Cl) assay in three different conditions (Figure 9c), which involves the use of the proton channel gramicidin D (Gra), and bovine serum albumin (BSA) (1 mol% with respect to lipid) treated vesicles.^[29] The addition of fatty acid (oleic acid, OA) to the NMDG-Cl assay allowed an evaluation of the receptors' ability to assist the flip-flop of the negatively charged fatty acid head group facilitating proton transport. BSA was used to sequester any fatty

acids present in the vesicles giving a fatty acid free lipid bilayer. The results of these thiophene-based molecules are presented in Figure S100-S123 and summarized in Table 2. As indicated by the factor of the chloride transport selectivity (F_{Gra}) quantified by dividing $EC_{50}(BSA)$ by $EC_{50}(Gra)$, these thiophene-based molecules only show a slight amount of chloride selective transport. Dividing $EC_{50}(BSA)$ by $EC_{50}(OA)$ give F_{OA} values > 1 for all receptors, indicating that all these receptors can couple fatty acid flip-flop and enhance the overall rate of H^+/Cl^- symport. Enhancement factors are greater or equal in the presence of OA compared to Gra, indicating the loss of the chloride transport selectivity in the presence of OA. The results demonstrate that these thiophene-based molecules preferentially facilitate H^+/Cl^- symport compared to uniport, reinforcing the electroneutral transport mechanism shown in the cationophore coupled assay.^[30]

Table 2. EC_{50} values shown for the *N*-methyl-D-glucamine chloride (NMDG-Cl) assay with bis-urea thiophene-based receptors in bovine serum albumin (BSA) treated vesicles, in the presence of gramicidin (Gra) and in the presence of oleic acid (OA).

Molecule	EC_{50} (mol %) ^a			Selectivity	
	BSA	Gra	OA	F_{Gra} ^b	F_{OA} ^c
4	0.0326	0.0272	0.0258	1.2	1.3
5	0.0237	0.0197	0.0184	1.2	1.3
7	0.0169	0.0094	0.0135	1.8	1.3
9	0.0039	0.0027	0.0028	1.4	1.4
11	0.0005	0.0005	0.0004	1.0	1.4
14	0.0334	0.0103	0.0072	3.2	4.6
15	0.0009	0.0004	0.0003	2.7	3.4
17	0.0021	0.0007	0.0007	3.1	3.2

^a) Values reported in transporter to lipid molar ratio (mol%); ^b) Factor of enhancement in the Cl^- uniport in the presence of Gra, F_{Gra} is calculated by dividing the $EC_{50}(BSA)$ by the $EC_{50}(Gra)$. $F_{Gra} > 1$ indicates Cl^- transport enhancement; ^c) Factor of enhancement in the overall rate of Cl^-/H^+ cotransport in the presence of OA, F_{OA} is calculated by dividing the EC_{50} by the $EC_{50}(OA)$. $F_{OA} > 1$ indicates the receptor can assist the flip-flop of OA, increasing pH dissipation.

Molecular dynamics simulations in a bilayer model

Further insights into the transport ability of our library of bis-urea derivatives were obtained through Molecular Dynamics (MD) simulations carried out with the chloride complexes of **3/4**, **8/9**, **14/15** and **16/17**, using AMBER18.^[31] These receptors were selected to ascertain how the molecular size, the binding geometry, and the fluorination of the central phenyl spacer affect their interaction and diffusion in the POPC bilayer system composed of 128 lipids and 6500 TIP3P water molecules. The receptors were described with the General AMBER Force Field,^[32] while lipid14^[33] was used for the POPC molecules. The complexes were placed either in the bilayer core or in the aqueous phase of the membrane model, affording the respective starting scenarios \mathcal{W} and \mathcal{L} , and simulated for 200 ns in two (**3**, **4**, **8**, and **9**) or three (**14-17**) independent MD runs. Remaining MD simulation details are given in ESI. The diffusion of the complexes was monitored tracking the distances between the closest bilayer interface (P_{int} , defined by the average *z* position of its 64 phosphorus atoms) and the centres of mass of the phenyl spacer (Ph_{COM} , defined by the six carbon atoms) and of the N-H binding

FULL PAPER

units ($N-H_{COM}$, defined by the four nitrogen atoms). The evolution of the $Ph_{COM}\cdots P_{int}$ and $N-H_{COM}\cdots P_{int}$ distances is plotted in Figures S124-S129, together with the counting of the $N-H\cdots Cl^-$ hydrogen bonds throughout the MD runs.

Regardless of the starting scenario, **W** or **L**, the bis-urea molecules diffuse towards the water/lipid interface. Indeed, even the ones coming from the water phase (**W**) permeate the interface and achieve equivalent positions as when they diffuse from the centre of the bilayer (**L**). Overall, the fluorinated molecules show a well-defined orientation along the MD simulations with the phenyl spacer and the N-H binding units closer to the bilayer core exposed to the water phase, respectively. In contrast, in the non-fluorinated analogous this orientation is less common, being swapped with ones where the receptor is tilted, with the N-H binding units away from the water phase. These dispositions are illustrated with two snapshots taken from the MD runs of **14** and **15**, in scenario **L** (see Figure 10).

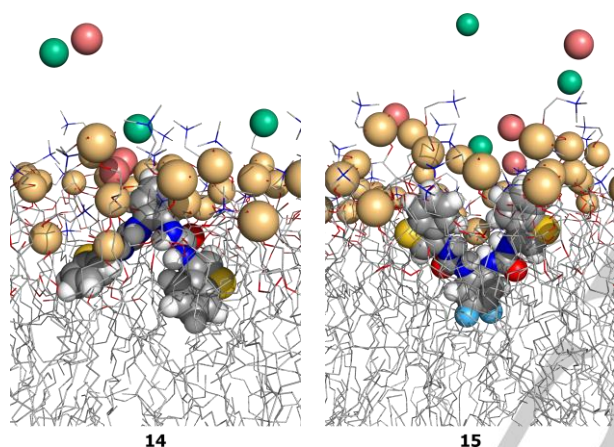


Figure 10. Snapshots of MD runs with **14** and **15** in scenario **L**, illustrating the opposite orientations acquired by the fluorinated and non-fluorinated receptors at the water/lipid interface. The water molecules and aliphatic protons were hidden for clarity.

Moreover, in the MD simulations in scenario **W**, the chloride is promptly hydrated, with the anion release preceding the bis-urea derivatives permeation of the bilayer. In contrast, in the alternative scenario **L**, as the complexes approach the water/lipid interface, the nearby water molecules promote the chloride release to the aqueous phase. Regardless of the starting scenario, as illustrated in Figure 11, with the counting of hydrogen bonds between **15** and Cl^- , phosphate head groups, *sn*-1 and *sn*-2 ester groups, and water molecules as a function of the position of the transporter along the bilayer normal (*z* axis), the $N-H\cdots Cl^-$ interactions are mainly replaced by hydrogen bonding interactions with the phosphate head groups (see Figures S130-S135 for the remaining MD runs). The high affinity of our small molecules for these hydrogen bonding acceptors (*vide infra*) might play an important role in their ability to promote the chloride transmembrane transport given that the anion uptake necessarily occurs at the water/lipid interface level, as we have previously demonstrated.^[27-28]

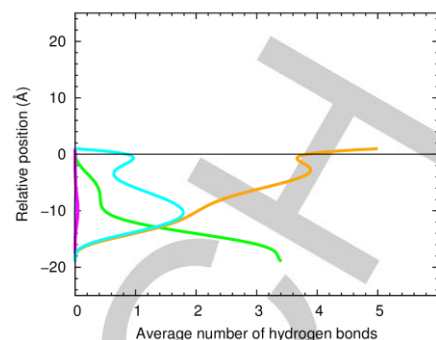


Figure 11. Average number of hydrogen bonds vs the relative position of the centre of mass of **15** in the second MD run in scenario **L**. The following colour scheme was used for the interactions between **15** and chloride ions (green), water molecules (cyan), POPC head groups (orange), and ester groups (magenta for the *sn*-1 chains and purple for the *sn*-2 chains). The water/lipid interface is represented as a black line at $z = 0$ Å.

The counting of $N-H\cdots Cl^-$ hydrogen bonds throughout the MD runs carried out in scenario **L** indicates that **3**, **4**, **14**, **8**, **9**, **16** and **17** typically release the anion within the first 50 ns of simulation. In contrast, in one of the initial MD runs of **15** the complex dissociation occurs almost at the end of the MD simulation (*ca.* 180 ns), which lead us to carry out two additional MD runs. In both simulations, the anion association was maintained throughout the 200 ns, suggesting that **15** has a higher affinity for chloride at the water/lipid interface of the POPC bilayer. Indeed, this insight is remarkable considering that the phenyl spacer is oriented to the bilayer core and that the complexed chloride is exposed to the competing water molecules amongst the phospholipid head groups. This result seems to be consistent with the high association constant of **15** for chloride in DMSO/H₂O (see Table 1), as well as its high anion efflux ability. On the other hand, **17** has the largest association constant for the halide, and lower transport properties. This intriguing result lead us to determine the association constants of the β - and γ -benzo[*b*]thiophenes (**14-17**) for $H_2PO_4^-$, as a prototype of the lipid head group. The association constants of these four molecules are extremely high, with the values for **14** and **15** being 11749 and 25119 M^{-1} , respectively, while for **16** and **17** the values are larger than $10^5 M^{-1}$.^[34] Thus, given that the two pairs of isomeric compounds have the same lipophilicities (see Table 1), the transport ability of **16** vs **14** and **17** vs **15** seems to be dictated by a delicate balance between their affinities for chloride and phosphate head groups. Therefore, **15**, with intermediate association constants for both anions, naturally emerges as the best transporter in this library of small molecules.

Cytotoxic screening

The cytotoxicity of the non-fluorinated/fluorinated analogous **3/4**, **8/9**, **14/15**, **16/17**, on HeLa, MCF-7 and A549 cancer cell lines was ascertained by the resazurin assay. These studies were further extended to CFBE cells, a human CF bronchial epithelial cell model, which has been used on functional studies of mutant CFTR in native context.^[35] These cells were exposed to different concentrations of compounds for 24 h yielding the IC_{50} values presented in Table 3.

FULL PAPER

Compounds **8**, **14**, **16** and **17** were found to be non-toxic towards all the cell lines tested. The remaining compounds were cytotoxic to some extent, with the fluorinated ones being the most toxic, as determined by the lower IC₅₀ values. In addition, the HeLa cells were the most sensitive line, with IC₅₀ values of 12.54 and 27.61 μM for **15**, and **4**, respectively, while **9** and **4** were particularly cytotoxic for the A549 cell line, with IC₅₀ values of 17.66 and 48.74 μM, respectively. Concerning the MCF-7 cells, only the α-thiophene derivatives show a moderate activity, with the fluorinated **4** displaying an IC₅₀ value (37.33 μM) that is almost half of its non-fluorinated analogous **3** (68.32 μM). In respect to the CFBE cell line, **3**, **4** and **9** display IC₅₀ values below 100 μM, while the most efficient transporter **15** has an IC₅₀ of 124.80 μM. This low cytotoxic level is significant considering the potential use of **15** as a Channel Replacement Therapy.

Table 3. IC₅₀ values (μM) for selected thiophene-based compounds on HeLa, MCF-7, A549 and CFBE cell lines.^a

Compound	HeLa	A549	MCF-7	CFBE
3	59.33	74.59	68.32	86.20
4	27.61	48.74	37.33	51.41
9	48.73	17.66	-	27.86
15	12.54	83.23	-	124.80

^a Compounds **8**, **14**, **16** and **17** have IC₅₀ values superior to 125 μM, being not reported.

Conclusions

Overall, the experimental binding data reported for the six-subsets (see Table 1) of thiophene based receptors show that the fluorination of the receptor skeleton increases the affinity for chloride. This finding mirrors the acidic character of the two urea-binding units ascertained by the V_{S,max} quantum descriptor as well as by the strength of the hydrogen bonding interactions estimated by E² energies. It is worth noting that the affinity of β-, and γ-benzo[b]thiophene derivatives for chloride significantly increase as result of a synergetic recognition by N-H...Cl⁻ and C-H...Cl⁻ hydrogen bonding interactions, as thoroughly documented by ¹H NMR data and theoretical calculations. Moreover, in these subsets the impact of the fluorination of the central phenyl spacer on the association constants is noticeable with the fluorinated analogous showing the higher values (163.7 M⁻¹ for **15** and 207.5 M⁻¹ for **17**) of our extensive library of small molecules. On the other hand, regardless of the fluorination of the aromatic spacer, the control of the receptors' conformation, through the C-H...O interactions, has a relevant role in the superior binding affinity of the β-, and γ-benzo[b]thiophene derivatives (**14-17**).

The most effective chloride transmembrane transporters are **15** and **17** followed by **14**, while **16**, the non-fluorinated analogous of **17**, is surprisingly almost inactive. Indeed, the anion efflux data obtained for fluorinated and non-fluorinated analogous of our library of small molecules indicates that the fluorination of the central ring potentiates the chloride transport across POPC bilayer. Accordingly, molecular dynamics simulations show that the fluorinated molecules reside below the bilayer interface with

the N-H binding units oriented towards the water phase prompt to uptake a chloride, as requested by the anion carrier mechanism. In contrast, the non-fluorinated analogous swap between multiple orientations and preferentially interact with phospholipid head groups, which necessarily limits their transport abilities as indicated by lower initial rates of chloride transport obtained for these molecules. Noteworthy, the chloride complex of **15** has longer lifetimes throughout the MD runs in the membrane system, which is consistent with its superior anion transport. The transport properties achieved with this library of molecules, inspired us to decorate other supramolecular scaffolds with sulfur heteroaromatic motifs. This project is ongoing in our laboratories.

Acknowledgements

The CFBE cell line was kindly provided by Prof. Margarida D. Amaral (Coordinator of BioISI – Biosystems & Integrative Sciences Institute, Department of Chemistry and Biochemistry, Faculty of Sciences, University of Lisbon). This work was supported by the projects PTDC/QEQ-SUP/4283/2014, UID/MULTI/00612/2019 and CICECO – Aveiro Institute of Materials (UID/CTM/50011/2019), financed by National Funds through the FCT/MEC and co-financed by QREN-FEDER through COMPETE under the PT2020 Partnership Agreement. M. M. is thankful for PhD grant PD/BD/142933/2018 from FCT. I.M. is grateful for a postdoctoral grant (BPD/UI98/6065/2018) under project “pAGE” (Centro-01-0145-FEDER-000003), co-funded by Centro 2020 programme, Portugal 2020, European Union, through the European Regional Development Fund. PAG thanks the ARC (DP180100612) and the University of Sydney for funding.

Keywords: Anion transport • thiophene-based molecules • efflux studies • molecular modelling • cytotoxicity

- [1] F. M. Ashcroft, *Ion Channels and Disease*, Vol. 1, 1st ed., Academic Press, London, **2000**.
- [2] B. P. O'Sullivan, S. D. Freedman, *The Lancet* **2009**, *373*, 1891-1904.
- [3] M. A. Ashlock, R. J. Beall, N. M. Hamblett, M. W. Konstan, C. M. Penland, B. W. Ramsey, J. M. Van Dalssen, D. R. Wetmore, P. W. Campbell, 3rd, *Semin. Respir. Crit. Care Med.* **2009**, *30*, 611-626.
- [4] E. J. Jeong, E. J. Kang, L. T. Sung, S. K. Hong, E. Lee, *J. Am. Chem. Soc.* **2002**, *124*, 14655-14662.
- [5] T. R. Sheth, R. M. Henderson, S. B. Hladky, A. W. Cuthbert, *Biochim. Biophys. Acta* **1992**, *1107*, 179-185.
- [6] S. Ohkuma, T. Sato, M. Okamoto, H. Matsuya, K. Arai, T. Kataoka, K. Nagai, H. H. Wasserman, *Biochem. J* **1998**, *334*, 731-741.
- [7] K. A. Muraglia, R. S. Chorghade, B. R. Kim, X. X. Tang, V. S. Shah, A. S. Grillo, P. N. Daniels, A. G. Cioffi, P. H. Karp, L. Zhu, M. J. Welsh, M. D. Burke, *Nature* **2019**, *567*, 405-408.
- [8] (a) P. A. Gale, E. N. W. Howe, X. Wu, M. J. Spooner, *Coord. Chem. Rev.* **2018**, *375*, 333-372; (b) X. H. Yu, X. Q. Hong, Q. C. Mao, W. H. Chen, *Eur. J. Med. Chem.* **2019**, *184*, 111782.
- [9] P. A. Gale, *Acc. Chem. Res.* **2011**, *44*, 216-226.
- [10] (a) J. L. Seganiash, J. T. Davis, *Chem. Commun.* **2005**, 5781-5783; (b) J. L. Sessler, L. R. Eller, W. S. Cho, S. Nicolaou, A. Aguilar, J. T. Lee, V. M. Lynch, D. J. Magda, *Angew. Chem. Int. Ed. Engl.* **2005**, *44*, 5989-5992; (c) P. Iglesias Hernandez, D. Moreno, A. A. Javier, T. Torroba, R. Perez-Tomas, R. Quesada, *Chem. Commun.* **2012**, *48*, 1556-1558; (d) V. Saggiomo, S. Otto, I. Marques, V. Félix, T. Torroba, R. Quesada, *Chem. Commun.* **2012**, *48*, 5274-5276.
- [11] (a) O. Jurček, H. Valkenier, R. Puttreddy, M. Novák, H. A. Sparkes, R. Marek, K. Rissanen, A. P. Davis, *Chem. Eur. J.* **2018**, *24*, 8178-8185; (b) D. H. Sohn, E. Han, J. I. Park, S. J. Cho, J. Kang, *Supramol. Chem.* **2018**, *30*, 169-178.

FULL PAPER

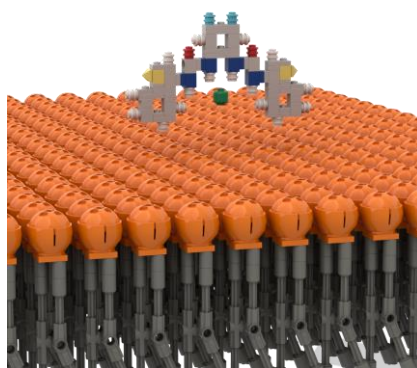
- [12] (a) A. V. Jentzsch, D. Emery, J. Mareda, S. K. Nayak, P. Metrangolo, G. Resnati, N. Sakai, S. Matile, *Nat. Commun.* **2012**, *3*, 905; (b) A. Vargas Jentzsch, A. Hennig, J. Mareda, S. Matile, *Acc. Chem. Res.* **2013**, *46*, 2791-2800; (c) A. Vargas Jentzsch, S. Matile, *J. Am. Chem. Soc.* **2013**, *135*, 5302-5303; (d) A. V. Jentzsch, S. Matile, *Top. Curr. Chem.* **2015**, *358*, 205-239.
- [13] (a) S. Benz, M. Macchione, Q. Verolet, J. Mareda, N. Sakai, S. Matile, *J. Am. Chem. Soc.* **2016**, *138*, 9093-9096; (b) M. Macchione, M. Tsemperouli, A. Goujon, A. R. Mallia, N. Sakai, K. Sugihara, S. Matile, *Helv. Chim. Acta* **2018**, *101*, e1800014; (c) L. M. Lee, M. Tsemperouli, A. I. Poblador-Bahamonde, S. Benz, N. Sakai, K. Sugihara, S. Matile, *J. Am. Chem. Soc.* **2019**, *141*, 810-814.
- [14] (a) L. Martinez-Crespo, J. L. Sun-Wang, P. Ferreira, C. F. M. Mirabella, G. Aragay, P. Ballester, *Chem. Eur. J.* **2019**, *25*, 4775-4781; (b) W. L. Huang, X. D. Wang, S. Li, R. Zhang, Y. F. Ao, J. Tang, Q. Q. Wang, D. X. Wang, *J. Org. Chem.* **2019**, *84*, 8859-8869.
- [15] H. Li, H. Valkenier, A. G. Thorne, C. M. Dias, J. A. Cooper, M. Kieffer, N. Busschaert, P. A. Gale, D. N. Sheppard, A. P. Davis, *Chem. Sci.* **2019**, *10*, 9663-9672.
- [16] (a) A. M. Rodilla, L. Korrodi-Gregorio, E. Hernando, P. Manuel-Manresa, R. Quesada, R. Perez-Tomas, V. Soto-Cerrato, *Biochem. Pharmacol.* **2017**, *126*, 23-33; (b) N. Busschaert, S. H. Park, K. H. Baek, Y. P. Choi, J. Park, E. N. W. Howe, J. R. Hiscock, L. E. Karagiannidis, I. Marques, V. Félix, W. Namkung, J. L. Sessler, P. A. Gale, I. Shin, *Nat. Chem.* **2017**, *9*, 667-675; (c) N. Akhtar, A. Saha, V. Kumar, N. Pradhan, S. Panda, S. Morla, S. Kumar, D. Manna, *ACS Appl Mater Interfaces* **2018**, *10*, 33803-33813; (d) R. Quesada, *Chem* **2019**, *5*, 1924-1926.
- [17] D. N. Sheppard, A. P. Davis, *Nature* **2019**, *567*, 315-317.
- [18] (a) D. Gramerc, L. Peterlin Masic, M. Sollner Dolenc, *Chem. Res. Toxicol.* **2014**, *27*, 1344-1358; (b) R. S. Keri, K. Chand, S. Budagumpi, S. Balappa Somappa, S. A. Patil, B. M. Nagaraja, *Eur. J. Med. Chem.* **2017**, *138*, 1002-1033.
- [19] W. M. Haynes, *CRC Handbook of Chemistry and Physics*, 97th ed., CRC Press LLC Taylor & Francis Group, Boca Raton; Florence, **2016**.
- [20] C. M. Dias, H. Valkenier, A. P. Davis, *Chem. Eur. J.* **2018**, *24*, 6262-6268.
- [21] (a) S. J. Moore, C. J. E. Haynes, J. Gonzalez, J. L. Sutton, S. J. Brooks, M. E. Light, J. Herniman, G. J. Langley, V. Soto-Cerrato, R. Perez-Tomas, I. Marques, P. J. Costa, V. Félix, P. A. Gale, *Chem. Sci.* **2013**, *4*, 103-117; (b) C. M. Dias, H. Li, H. Valkenier, L. E. Karagiannidis, P. A. Gale, D. N. Sheppard, A. P. Davis, *Org. Biomol. Chem.* **2018**, *16*, 1083-1087.
- [22] J. Tomasi, B. Mennucci, R. Cammi, *Chem. Rev.* **2005**, *105*, 2999-3093.
- [23] Gaussian 09, M. J. Frisch, G. W. Trucks, H. B. Schlegel, G. E. Scuseria, M. A. Robb, J. R. Cheeseman, G. Scalmani, V. Barone, B. Mennucci, G. A. Petersson, H. Nakatsuji, M. Caricato, X. Li, H. P. Hratchian, A. F. Izmaylov, J. Bloino, G. Zheng, J. L. Sonnenberg, M. Hada, M. Ehara, K. Toyota, R. Fukuda, J. Hasegawa, M. Ishida, T. Nakajima, Y. Honda, O. Kitao, H. Nakai, T. Vreven, J. A. Montgomery, Jr., J. E. Peralta, F. Ogliaro, M. Bearpark, J. J. Heyd, E. Brothers, K. N. Kudin, V. N. Staroverov, R. Kobayashi, J. Normand, K. Raghavachari, A. Rendell, J. C. Burant, S. S. Iyengar, J. Tomasi, M. Cossi, N. Rega, J. M. Millam, M. Klene, J. E. Knox, J. B. Cross, V. Bakken, C. Adamo, J. Jaramillo, R. Gomperts, R. E. Stratmann, O. Yazyev, A. J. Austin, R. Cammi, C. Pomelli, J. W. Ochterski, R. L. Martin, K. Morokuma, V. G. Zakrzewski, G. A. Voth, P. Salvador, J. J. Dannenberg, S. Dapprich, A. D. Daniels, O. Farkas, J. B. Foresman, J. V. Ortiz, J. Cioslowski, and D. J. Fox, Gaussian, Inc., Wallingford CT, 2009.
- [24] (a) F. Weinhold, C. R. Landis, *Chem. Educ. Res. Pract.* **2001**, *2*, 91-104; (b) E. D. Glendening, C. R. Landis, F. Weinhold, *J. Comput. Chem.* **2013**, *34*, 1429-1437.
- [25] Calculator Plugins were used for structure property prediction and calculation, Marvin Sketch 19.2.0-9405, 2019, ChemAxon (<http://www.chemaxon.com>).
- [26] C. Frassinetti, S. Ghelli, P. Gans, A. Sabatini, M. S. Moruzzi, A. Vacca, *Anal. Biochem.* **1995**, *231*, 374-382.
- [27] M. J. Spooner, H. Li, I. Marques, P. M. R. Costa, X. Wu, E. N. W. Howe, N. Busschaert, S. J. Moore, M. E. Light, D. N. Sheppard, V. Félix, P. A. Gale, *Chem. Sci.* **2019**, *10*, 1976-1985.
- [28] I. Marques, P. M. R. Costa, Q. M. M. N. Busschaert, E. N. W. Howe, H. J. Clarke, C. J. E. Haynes, I. L. Kirby, A. M. Rodilla, R. Perez-Tomas, P. A. Gale, V. Félix, *Phys. Chem. Chem. Phys.* **2018**, *20*, 20796-20811.
- [29] X. Wu, L. W. Judd, E. N. W. Howe, A. M. Withecombe, V. Soto-Cerrato, H. Li, N. Busschaert, H. Valkenier, R. Perez-Tomas, D. N. Sheppard, Y. B. Jiang, A. P. Davis, P. A. Gale, *Chem* **2016**, *1*, 127-146.
- [30] X. Wu, J. R. Small, A. Cataldo, A. M. Withecombe, P. Turner, P. A. Gale, *Angew. Chem. Int. Ed. Engl.* **2019**, *58*, 15142-15147.
- [31] D. A. Case, I. Y. Ben-Shalom, S. R. Brozell, D. S. Cerutti, T. E. Cheatham, III, V. W. D. Cruzeiro, T. A. Darden, R. E. Duke, D. Ghoreishi, G. Giambasu, T. Giese, M. K. Gilson, H. Gohlke, A. W. Goetz, D. Greene, R. Harris, N. Homeyer, Y. Huang, S. Izadi, A. Kovalenko, R. Krasny, T. Kurtzman, T. S. Lee, S. LeGrand, P. Li, C. Lin, J. Liu, T. Luchko, R. Luo, V. Man, D. J. Mermelstein, K. M. Merz, Y. Miao, G. Monard, C. Nguyen, H. Nguyen, A. Onufriev, F. Pan, R. Qi, D. R. Roe, A. Roitberg, C. Sagui, S. Schott-Verdugo, J. Shen, C. L. Simmerling, J. Smith, J. Swails, R. C. Walker, J. Wang, H. Wei, L. Wilson, R. M. Wolf, X. Wu, L. Xiao, Y. Xiong, D. M. York and P. A. Kollman (2018), AMBER 2018, University of California, San Francisco.
- [32] (a) J. Wang, R. M. Wolf, J. W. Caldwell, P. A. Kollman, D. A. Case, *J. Comput. Chem.* **2004**, *25*, 1157-1174; (b) J. Wang, R. M. Wolf, J. W. Caldwell, P. A. Kollman, D. A. Case, *J. Comput. Chem.* **2005**, *26*, 114-114.
- [33] C. J. Dickson, B. D. Madej, A. A. Skjevik, R. M. Betz, K. Teigen, I. R. Gould, R. C. Walker, *J. Chem. Theory Comput.* **2014**, *10*, 865-879.
- [34] H₂PO₄⁻ added as TBA salt and the binding constants were determined by ¹H NMR titrations in DMSO-d₆/0.5% H₂O at 293 K using HypNMR. The remaining molecules deprotonated in presence of H₂PO₄⁻.
- [35] L. B. Gottschalk, B. Vecchio-Pagan, N. Sharma, S. T. Han, A. Franca, E. S. Wohler, D. A. Batista, L. A. Goff, G. R. Cutting, *J. Cyst. Fibros* **2016**, *15*, 285-294.

FULL PAPER

Entry for the Table of Contents

FULL PAPER

A library of drug-like molecules, containing thiophene and benzo[*b*]thiophene motifs, was designed for the transmembrane transport of chloride. The theoretical and experimental investigation showed, that the most active ones operate the anion transport *via* a symport mechanism and taking advantage of the synergy between N-H...Cl⁻ and C-H...Cl⁻ hydrogen bonds.



Paulo Vieira, Margarida Q. Miranda, Igor Marques, Sílvia Carvalho, Li-Jun Chen, Ethan N. W. Howe, Carl Zhen, Claudia Y. Leung, Michael J. Spooner, Bárbara Morgado, Odete A. B. da Cruz e Silva, Cristina Moiteiro, Philip A. Gale,* Vítor Félix**

Page No. – Page No.

Development of a library of thiophene-based drug-like LEGO molecules: evaluation of their anion binding, transport properties and cytotoxicity

WILEY

Accepted Manuscript